




# Tumor-derived exosomes drive pre-metastatic niche formation in lung via modulating CCL1<sup>+</sup> fibroblast and CCR8<sup>+</sup> Treg cell interactions

Ming Wang<sup>1</sup> · Zhongyu Qin<sup>2</sup> · Jiajia Wan<sup>1</sup> · Yan Yan<sup>1</sup> · Xixi Duan<sup>1</sup> · Xiaohan Yao<sup>1</sup> · Ziming Jiang<sup>3</sup> · Wenqing Li<sup>1</sup> · Zhihai Qin<sup>1,4</sup> 

Received: 5 January 2022 / Accepted: 25 March 2022 / Published online: 15 April 2022  
© The Author(s), under exclusive licence to Springer-Verlag GmbH Germany, part of Springer Nature 2022

## Abstract

**Background** Since the lung is one of the most common sites for cancer metastasis, it could provide a suitable microenvironment for pre-metastatic niche (PMN) formation to facilitate tumor cell colonization. Regulatory T cells (Tregs) are an immunosuppressive cell type found ubiquitously in tumors and may play a crucial role in PMN formation. In this study, we investigated tumor-derived exosome (TDE)-induced Treg differentiation in the lung PMN as well as the underlying mechanisms.

**Methods** TDEs were isolated from the Lewis lung carcinoma cell line (LLC-exo) and their effects on mouse pulmonary fibroblasts was investigated in vitro as well as on lung tumor formation and metastasis in a pre-injected mouse model. Immune cell populations in the lung were analyzed by flow cytometry. Expression of CCL1 and CCR8 was evaluated by immunofluorescence staining, qRT-PCR and Western blot analyses. Cytokine expression was measured using mouse cytokine arrays and ELISA.

**Results** The number of CD4<sup>+</sup> FoxP3<sup>+</sup> Tregs was significantly increased in lungs in a LLC-exo pre-injected mouse model. Lung fibroblasts secreted increased amounts of CCL1 after co-culture with LLC-exo, which induced Treg differentiation by activating its specific receptor CCR8, ultimately contributing to the establishment of an immunologically tolerant PMN. Moreover, inhibiting the release of LLC-exo by GW4869, or blocking the CCL1-CCR8 axis using AZ084, suppressed Tregs differentiation and tumor metastasis in the lung.

**Conclusions** Collectively, our study provides a novel mechanism by which Tregs are activated to form an immunologically tolerant PMN and demonstrates a critical link among lung fibroblasts, Tregs and metastatic tumor cells.

**Keywords** Metastasis · PMN · Fibroblasts · Tregs · CCL1–CCR8

---

Ming Wang and Zhongyu Qin have contributed equally to this work.

---

✉ Ming Wang  
wangmingheda@163.com

✉ Zhihai Qin  
zhihai@ibp.ac.cn

Zhongyu Qin  
1830418498@qq.com

Jiajia Wan  
wjy123@mail.ustc.edu.cn

Yan Yan  
yy263216342@163.com

Xixi Duan  
duanxixi90@163.com

Xiaohan Yao  
yxhzzu@163.com

Ziming Jiang  
17865198202@163.com

Wenqing Li  
1500116808@qq.com

<sup>1</sup> Medical Research Center, The First Affiliated Hospital of Zhengzhou University, Zhengzhou University, Zhengzhou 450052, Henan, China

<sup>2</sup> Changzhi Medical College, Changzhi 046000, Shanxi, China

<sup>3</sup> Department of Urology, The First Affiliated Hospital of Zhengzhou University, Zhengzhou 450052, Henan, China

<sup>4</sup> Academy of Medical Sciences, Zhengzhou University, Zhengzhou 450052, Henan, China

## Abbreviations

CAF	Cancer-associated fibroblasts
DMED	Dulbecco's Modified Eagle's Medium
ECM	Extracellular matrix
EV	Extracellular vesicles
FBS	Fetal bovine serum
HE	Hematoxylin and eosin
LLC-exo	Lewis lung carcinoma exosome
MDSCs	Myeloid-derived suppressor cells
MPF	Mouse pulmonary fibroblasts
PMN	Pre-metastatic niche
RBC	Red blood cells
TDE	Tumor cell-derived exosomes
TME	Tumor microenvironment
Tregs	Regulatory T cells

## Introduction

Tumor metastases are responsible for more than 90% of cancer-associated deaths [1, 2]. According to the proposed “seed and soil” hypothesis for tumor metastasis, the metastatic site provides a favorable microenvironment for immunosuppression, inflammation, and angiogenesis, that supports circulating tumor cell engraftment and growth [3–5]. This microenvironment established prior to tumor metastasis is also referred as the pre-metastatic niche (PMN) [6, 7]. The lung is one of the most common sites of cancer metastasis, occurring in more than half of metastatic solid cancer patients. Therefore, understanding the mechanism of PMN formation in the lung is a topic of great clinical importance, which will also provide insights into the development of novel therapeutic approaches to inhibit tumor metastasis to the lung.

Formation of the PMN is believed to be influenced by the primary cancer cells even before the initiation of metastasis [8, 9]. The PMN develops via a multistep process including vascular leakage, extracellular matrix (ECM) remodeling and immunosuppressive ambience [7, 10]. The immunosuppressive microenvironment protects tumor cells from host immune attack at the metastatic sites, which is a key step in tumor cell metastasis. Regulatory T cells (Tregs) are one of the most notable immunosuppressive immune cells within the PMN [11]. Tregs play an important role in regulation of immune homeostasis and self-tolerance, which also attenuate anti-tumor immunity and promote tumor metastasis [12, 13]. Tregs have been reported to facilitate breast cancer cell lung metastasis by killing natural killer cells through expression of  $\beta$ -galactosidase-binding protein, which neutralizes their ability to eliminate tumor cells [14]. However, the mechanism by which Tregs are polarized and accumulate in the PMN remains to be elucidated.

According to one of the proposed mechanisms, PMN formation is achieved by secretory factors and extracellular vesicles (EV) derived from tumor cells [8, 15]. Exosomes, which are the most intensively studied subtype of EV, transfer invasion-promoting factors to metastatic sites and contribute to the establishment of the PMN [10, 16]. For instance, pancreatic tumor cell-derived exosomes (TDEs) assist tumor cell metastasis by activating stromal fibroblasts and establishing a pre-metastatic tumor microenvironment (TME) [17, 18]. Lung TDEs upregulate macrophages PD-L1 expression and promote lung PMN formation to facilitate tumor cell metastatic colonization to lung [19]. Moreover, exosome-derived factors activate epidermal growth factor receptor signaling to support tumor cell invasion, induce angiogenesis and provide nutrients for metastatic tumor cell growth [20, 21]. In addition, TDEs have been reported to impede anti-tumor immune responses by transferring their immunosuppressive cargo or mediating myeloid-derived suppressor cell (MDSCs) differentiation [22, 23]. TDE-mediated Treg accumulation in the tumor stroma has been reported in cancers including lung cancer and breast cancer. Nevertheless, whether TDEs play a role in the induction of Treg differentiation and accumulation in the PMN is still unclear.

In our previous study, we demonstrated that most exosomes derived from lung tumor cells are taken up by lung fibroblasts and induce pro-inflammatory cytokine gene expression [24]. These findings further prompt us to explore the effect of the increased cytokines in the lung on the number of Tregs in TDE pre-treated mouse lung as well as the circulating tumor cell lung colonization. In this study, we investigated the effects of TDE-educated fibroblasts on Treg differentiation and formation of the immunologically tolerant PMN in the lungs.

## Methods

### Cell lines and cell culture

The Lewis lung carcinoma cell line (LLC) was provided by Professor Li Yan from the Academy of Military Medical Sciences (China, Beijing). Dulbecco's Modified Eagle's Medium (DMEM, HyClone, Marlborough, MA, USA) supplemented with additional 10% of Hyclone fetal bovine serum (FBS, Gibco, Waltham, MA, USA) and 1% penicillin–streptomycin solution (Hyclone) were used for cell culture. All cells were maintained at 37 °C in a humidified incubator under 5% CO<sub>2</sub>.

## Animals

Female C57BL/6 J mice (aged 6–8 weeks) were purchased from the Vital River Laboratory Animal Technology Company (Beijing, China). All mice were housed in individually ventilated cages on racks in a specific pathogen-free facility with controlled temperature (20–25 °C) and humidity (40–60%).

## Primary lung fibroblast isolation

Primary lung fibroblasts were isolated from 7-day-old C57BL/6 J mice. Briefly, the dissected lungs were washed with sterile phosphate-buffered saline (PBS; Hyclone), then cut into small pieces (approximately 1 mm<sup>3</sup>) and washed again with PBS. Subsequently, the tissue was resuspended in 2 ml complete DMEM and incubated in a 10 cm tissue culture dish overnight. After adding another 10 ml medium and removing the unattached pieces, the remaining lung fragments were cultured in complete DMEM, with the medium changed every 2 days to allow the fibroblasts to exit the tissue and attach to the plate. After the fibroblasts reached 90% confluence, an aliquot of cells was frozen for subsequent experiments.

## Splenic T cell isolation and co-culture experiment

Splenic T cells were isolated from female C57BL/6 J mice. The spleen was washed with sterile PBS and then transferred to a 6 cm tissue culture dish. A single cell suspension was prepared from the spleen by injecting 5 ml PBS, followed by dissection and passing through a 70- $\mu$ m filter (BD Bioscience, FL, USA). The red blood cells (RBC) were removed using RBC lysis buffer (Solarbio, Beijing, China). After washing with PBS, the pellet was resuspended, and  $1 \times 10^5$  cells were seeded in 6-well culture plates (Corning, NY, USA). After 60 min, the unattached T cells were collected for co-culture experiments. The LLC-exo treated mouse pulmonary fibroblast culture medium (LLC-exo MPF CM) was collected, filtered with 0.22  $\mu$ m filter (BD Bioscience), and then added to freshly isolated splenic T cells every day, with/without the CCL1-CCR8 blocker ZK756326 (Selleckchem, S8324) or the CCR8 inhibitor AZ084 (MCE, HY-119217). The percentage of Tregs was examined after 4 days.

## TDEs isolation and identification

LLC-exo were isolated by ultracentrifugation. At 90% confluence, LLC cells were washed with PBS and incubated with FBS-free medium for 24 h. The LLC supernatant was collected and centrifuged at  $200 \times g$  for 10 min and then  $20,000 \times g$  for 20 min, to remove the dead cells and cell debris. LLC-exo were then obtained by ultracentrifugation at

$100,000 \times g$  for 70 min. The mixed protein components were washed with PBS and purified LLC-exo were obtained after repeating the ultracentrifugation at  $100,000 \times g$  for 70 min. Purified LLC exosomes were identified by transmission electron microscopy (HT7800, HITACHI) and Western blot analysis of expression of the surface marker CD63. The size distribution of LLC-exo was determined by Malvern Zeta-sizer instrument (Version 7.04).

## TDEs tracing experiment

To track the LLC-exo uptake in vivo, we stained LLC-exo (10  $\mu$ g in 100  $\mu$ l PBS) with Cy5.5 (0.3  $\mu$ M, Fanbo Biochemicals, #1056) for 30 min at 37 °C. Following, the labeled LLC-exo were intravenously injected into C57BL/6 J mice for 12 h. Then the organs including lung, brain, spleen and liver were harvested and digested with collagenase D (1 mg/ml, Sigma-Aldrich, COLLD-RO) for 30 min at 37 °C. The single cell suspension was stained with Cd11b (FITC, BD Bioscience, 553,310, 1:100) and  $\alpha$ -SMA (1:100, CST, 19245 s). The proportion Cy5.5<sup>+</sup> cells in each organ were detected by flow cytometry (BD FACSCanto).

## RNA extraction and qRT-PCR

Total RNA was extracted from LLC-exo stimulated fibroblasts using TRIzol® reagent (TaKaRa, Shiga, Japan), and cDNA was prepared by reverse transcription with SYBR Green PCR Master Mix (RR036A; Takara, Tokyo, Japan) according to the manufacturer's instructions. qRT-PCR analysis of *Ccl1* expression was performed using specific primers (F: TGCCGTGTGGATACAGGATG; R: GTTGAG GCGCAGCTTTCTCTA) on the StepOnePlus detection system (ThermoFisher). The relative expression level of *Ccl1* was calculated by the  $2^{-\Delta\Delta C_t}$  method. Relative expression of *Ccl1* was normalized with *Gapdh* (F: TCTCTGCTCCTC CCTGTTCC; R: TACGGCCAAATCCGTTTACA). Each experiment was repeated three times.

## Flow cytometric analysis

To analyze the immune cell population after LLC-exo injection, the lungs were dissected, cut into small pieces (approximately 1 mm<sup>3</sup>), followed with incubation with 1 mg/ml collagenase D at 37 °C for 30 min. The tissue fragments were then filtered through a stainless-steel cell strainer (200- $\mu$ m mesh) (Solarbio). The RBCs were removed using RBC lysis buffer and the single cell suspension was stained with fluorochrome-conjugated antibodies for the detection of the following: CD45-Alexa Fluor700 (BioLegend, 104,115, 1:100) B220-APC (BD Bioscience, 553,092, 1:100), CD4-APC/Cy7 (BioLegend, 100,414, 1:100), Ly6G/C-PE (BD Bioscience, 553,128, 1:100), and FOXP3-FITC (BioLegend,

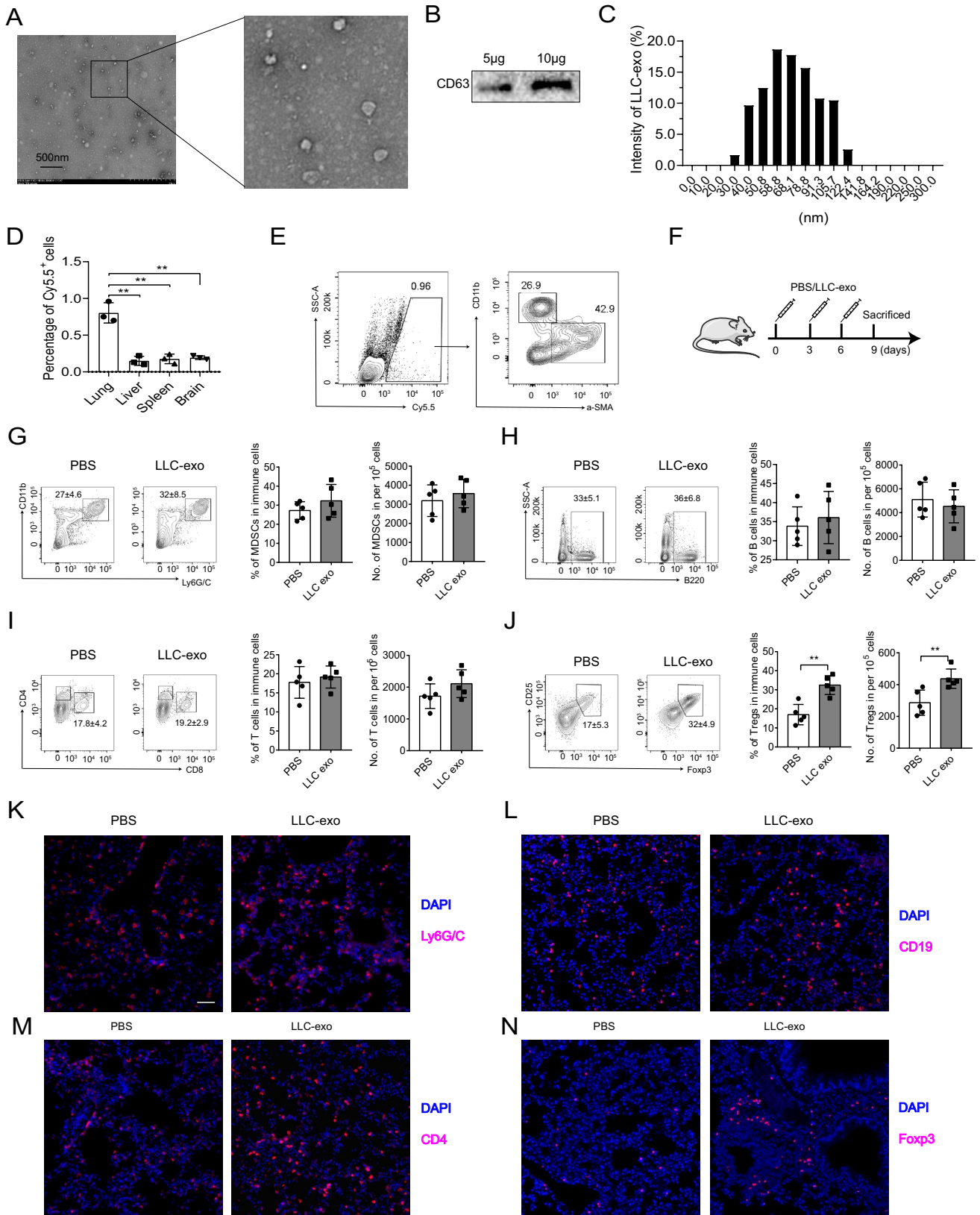


**Fig. 1** LLC-exo promote the accumulation of Tregs in mouse lung. **A** LLC-exo were isolated and observed by transmission electron microscopy; scale bar, 500 nm. **B** Expression of the LLC-exo surface marker CD63 was detected by Western blot analysis; **C** The size distribution of LLC-exo was analyzed by Malvern Zetasizer instrument. **D** The percentage of cy5.5<sup>+</sup> cells in total number of lung, liver, spleen and brain cells were determined by flow cytometry. **E** Flow cytometric analysis examined the uptake of cy5.5-labelled LLC-exo in CD11b<sup>+</sup> macrophages or  $\alpha$ -SMA<sup>+</sup> fibroblasts. **F** Schematic diagram of LLC-exo injection experiments; mice were injected with LLC-exo (10  $\mu$ g in 100  $\mu$ l PBS) or an equal volume of PBS every three days via the tail vein. The mice were then sacrificed and the lungs were isolated. **G–J** Flow cytometry analyzed the immune cell populations (CD45<sup>+</sup>CD11b<sup>+</sup>Ly6G/C<sup>+</sup> MDSCs, CD45<sup>+</sup>B220<sup>+</sup> B cells, CD4<sup>+</sup>/CD8<sup>+</sup> T cells and CD25<sup>+</sup>Foxp3<sup>+</sup> Tregs) in lungs ( $n=5$ ). **K–N** Evaluation of the number of immune cells in lung based on immunofluorescence staining of specific markers (Ly6G, CD19, CD4 and FoxP3); scale bar, 100  $\mu$ m. Data represent the mean  $\pm$  SD. \*\* $P < 0.01$  (Student's *t*-test)

126,406, 1:100). After washing with 1% BSA, the cells were analyzed by flow cytometry (BD FACSCanto, Franklin Lakes, NJ, USA), and data were analyzed by FlowJo X (Tree Star, Ashland, OR, USA) software.

### Immunofluorescence staining

For immune cell staining, frozen lung Sects. (6  $\mu$ m) were stained with the following anti-mouse antibodies: Ly6G/C-PE (BD Bioscience, 553,128, 1:100), B220 (CST, 34399 s, 1:200), CD4 (Abcam, ab183685, 1:200) and FOXP3 (CST, 12653 s, 1:100). To detect CCL1 and CCR8 expression in the lung or fibroblasts, lung sections were stained overnight at 4 °C with the following primary antibodies: CCL1 (RD system, MAB8451-SP, 1:300), CCR8 (ABclonal, A4288, 1:200) and  $\alpha$ -SMA (Abcam, ab5694, 1:200). Sections were then stained for 1 h at 4 °C with the AlexaFluor 488 (Thermo, A21206, 1:1,000) or AlexaFluor 555 (Thermo, A21434, 1:1,000)-conjugated secondary antibody. The nuclei were stained with DAPI (AR1176, Boster, Pleasanton, CA, USA). The sections were visualized with a laser scanning immunofluorescence microscope (Vectra 3.0, PerkinElmer).

### Western blot analysis

Lung fibroblasts or LLC exosomes were lysed with RIPA lysate buffer (Sigma) and protein concentrations were determined using the bicinchoninic acid (BCA) protein assay (Thermo Fisher Scientific). Total proteins (30  $\mu$ g) were separated by sodium dodecyl sulfate polyacrylamide gel electrophoresis and transferred to PVDF membranes (0.45  $\mu$ m, Sigma, 3,010,040,001). The membrane was blocked with 5% nonfat dried milk for 1 h and then incubated overnight at 4 °C with primary antibodies for detection of the following: CCR8 (ABclonal, A4288, 1:300), CD63 (Santa Cruz,

1:500, sc-5275) and  $\beta$ -actin (Abcam, 1:1,000, ab8227). The membrane was then incubated for 1 h at room temperature with horseradish peroxidase-conjugated secondary antibody (Proteintech, Rosemont, IL, USA, 1:2000, SA00001-9). Protein bands were visualized using an enhanced chemiluminescence kit (Thermo Fisher Scientific, USA) and quantified by densitometry using the ChemiDoc MP imaging system (BIO-RAD, USA).

### Mouse cytokine arrays

Lung fibroblasts were stimulated with LLC-exo for 24 h. After washing with PBS, the cells were then cultured in serum-free medium. After 24 h, the culture supernatant was collected and filtered (0.22  $\mu$ m; Merck Millipore) prior to incubation for 2 h at room temperature with the Mouse Cytokine Array (ARY006, RD, CA, USA). The array was then incubated with streptavidin–horseradish peroxidase secondary antibody (RD, 893,019, 1:1000) followed by chemiluminescent detection (ARY006 contained).

### ELISA

To confirm LLC-exo induced lung fibroblasts CCL1 protein concentration. A specific mouse CCL1 ELISA kit (RD, DY845) was used to measure the concentration of LLC-exo stimulated (24 h) fibroblasts supernatant, according to the manufacturer's instructions.

### Animal experiments

To explore the effect of LLC-exo on Treg accumulation as well as LLC cell colonization of lungs, C57BL/6 J mice were injected via the tail vein with LLC-exo combined with either CCL1-CCR8 blocker ZK756326 (10 mg/kg) or CCR8 antagonist AZ084 (5 mg/kg) every third day followed by  $5 \times 10^5$  LLC cells via the same route. After 21 days, the LLC cell colonization of the lung was detected by hematoxylin and eosin (HE) staining and the immune cell populations were analyzed by flow cytometry. To investigate the influence of primary LLC-exo on colonization of the lungs by circulating tumor cells, we established a subcutaneous LLC tumor model following treatment with GW4869 (MedChem-Express, HY-19363, 10 mg/kg) and AZ084. On day 15, the primary tumors were surgically removed and mice were injected  $5 \times 10^5$  LLC cells via the tail vein. The metastatic lung colonization was evaluated at day 36.

### Statistical analysis

All statistical analysis was performed using GraphPad Prism 8 software. In vitro experiments were conducted at least three times and data were displayed as mean  $\pm$  SD.



Statistical significance was evaluated using Student's *t*-test or one-way ANOVA.  $P < 0.05$  was set as the threshold for statistical significance.

## Results

### LLC-exo increase Foxp3<sup>+</sup> Treg accumulation in the lungs

In our previous study, we observed that LLC-exo promoted the cytokine genes expression in lung fibroblasts [24]. In the present study, we further investigated the role of fibroblast-derived cytokines on the accumulation of immune cells in the lungs. To accomplish this, the isolated LLC-exo were verified by transmission electron microscopy showing the typical cup-shaped morphology (Fig. 1A) and the expression of the surface marker CD63 (Fig. 1B) as well as the 30–100 μm size distribution (Fig. 1C). It has been proved that exosomes can home to tissues from their parent cell line of origin [16]. Our exosome tracking experiments confirmed that majority of LLC-exo were up taken by lung cells, particularly α-SMA<sup>+</sup> fibroblasts (Fig. 1D, E). Next, we investigated the immune cell populations in the lungs of mice following three intravascular injections of LLC-exo (Fig. 1F). The numbers of MDSCs (CD11b<sup>+</sup>Ly6G/C<sup>+</sup>), B cells (B220<sup>+</sup>) and T cells (CD4<sup>+</sup> and CD8<sup>+</sup>) (Fig. 1G–J) in the LLC-exo injection group were comparable with those in the sham control group. Interestingly, the immunosuppressive Treg (CD4<sup>+</sup> Foxp3<sup>+</sup>) population increased two-fold in the lungs of mice pre-injected with LLC-exo (J). These immune cell populations were further verified by fluorescence microscopy analysis (Fig. 1K–N). These data suggested that the exogenously administered LLC-exo promoted Treg accumulation in the lung.

### LLC-exo upregulate CCL1 secretion by lung fibroblasts

We next investigated which factor in LLC-exo stimulated fibroblasts has the potential to induce the accumulation of Foxp3<sup>+</sup> Tregs in the lung. Using a mouse cytokine array kit, we showed that LLC-exo treated lung fibroblasts secrete several chemokines including CXCL1, CCL5 and CCL1. Among the altered cytokines, CCL1 was the most significantly upregulated factors at both the protein and mRNA levels (Fig. 2A–C). Moreover, we also detected the increased co-localization of CCL1 with α-SMA<sup>+</sup> fibroblasts in LLC-exo pre-injected mouse lungs. These data indicated that the LLC-exo promote CCL1 expression in lung fibroblasts (Fig. 2D).

### CCL1 derived from LLC-exo stimulated fibroblasts plays a key role in inducing Treg differentiation

Having shown that LLC-exo promote CCL1 production by lung fibroblasts, we next investigated the ability of CCL1 produced by LLC-exo treated lung fibroblasts to promote Treg differentiation in vitro. For this purpose, we treated splenic T cells with LLC-exo stimulated mouse pulmonary fibroblast culture medium (LLC-exo MPF CM group) for 4 days. Intriguingly, the proportion of Tregs in CD4<sup>+</sup> T cells in the LLC-exo MPF CM group was approximately two-fold greater than that in the control group. CCL1 has been reported to induce Treg differentiation via its receptor CCR8 [25]. Therefore, we used ZK756326 to inhibit the binding of CCL1 to CCR8 in order to verify the role of fibroblast-derived CCL1 plays in inducing Treg differentiation. As expected, ZK756326 treatment suppressed the induction of Treg differentiation by LLC-exo MPF CM (Fig. 3B, C). Similarly, the increased proportion of CD4<sup>+</sup>FoxP3<sup>+</sup> Tregs in LLC-exo pre-treated lung in vivo was reversed by additional ZK756326 treatment (Fig. 3D–G). Taken together, our findings demonstrated that CCL1 derived from LLC-exo treated fibroblasts plays a key role in inducing Treg differentiation both in vitro and in vivo.

### Blockade of CCR8 inhibits Treg differentiation in vitro and in vivo

We next investigated the role of the CCL1-CCR8 axis in Treg differentiation in the lung. First, we observed that the CCR8 expression by splenic T cells was significantly upregulated after in vitro culture with LLC-exo MPF CM (Fig. 4A). Similarly, the co-localization of CCR8 with Foxp3<sup>+</sup> was also increased in the lungs of LLC-exo pre-treated mice (Fig. 4B). We then used AZ084, a CCR8 antagonist, to further confirm the important role of the CCL1-CCR8 interplay in Treg differentiation. AZ084 treatment reversed the increased proportion of Tregs among the CD4<sup>+</sup> T cells co-cultured in vitro with LLC-exo MPF CM (Fig. 4C–E). Similarly, CCR8 expression T cells cultured in vitro with by LLC-exo MPF CM was reduced in the presence of AZ084 (Fig. 4F). Moreover, the total numbers of Tregs and CCR8<sup>+</sup> Tregs in the lungs of LLC-exo pre-treated mice was reduced when combined with AZ084 treatment (Fig. 4G, H). Collectively, these data indicated that the interplay between CCR8 on T cells and its ligand CCL1 derived from fibroblasts plays a critical role in Treg differentiation.

### Targeting CCR8 suppresses lung colonization by circulating LLC cells

We next explored the possibility that targeting the CCL1-CCR8 mediated fibroblast-Treg crosstalk could restrain

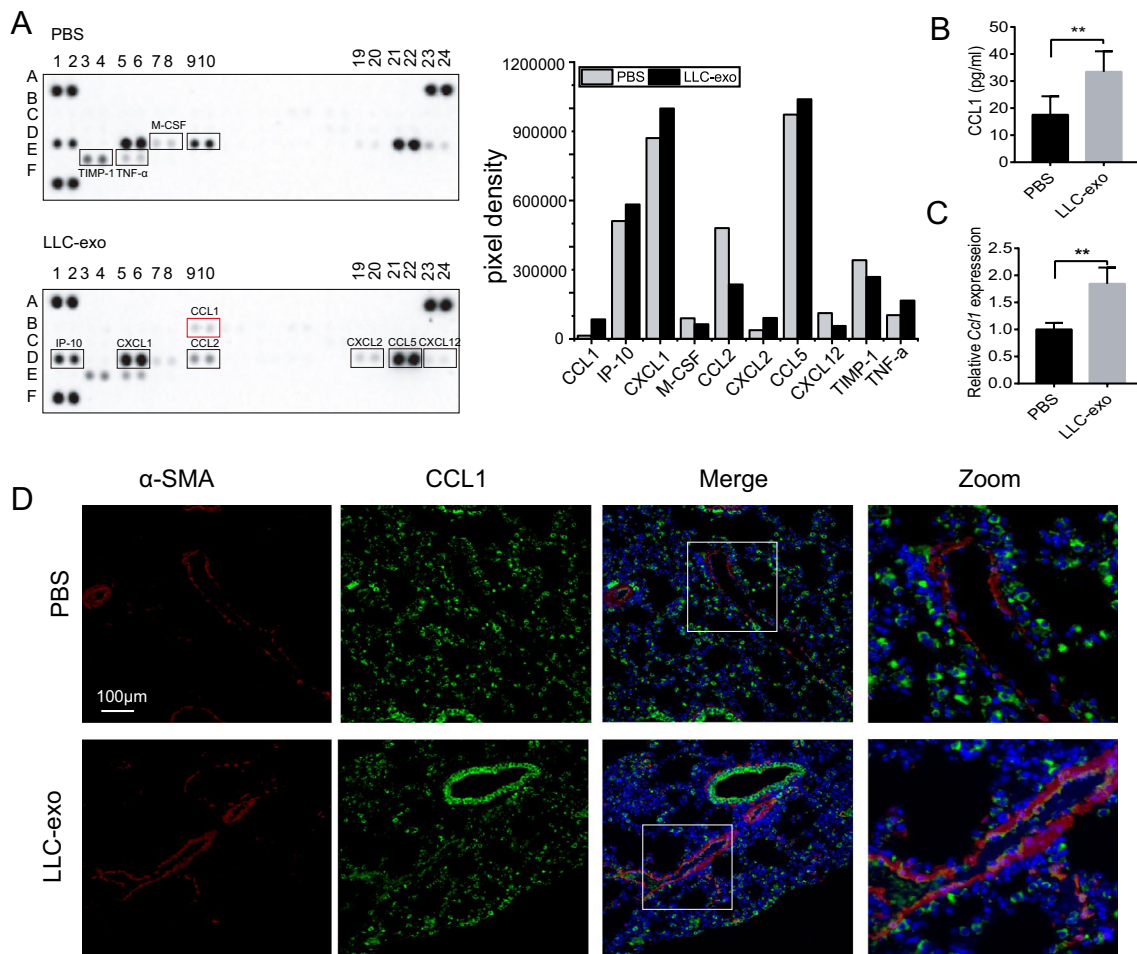


**Fig. 2** LLC-exo upregulate CCL1 secretion by lung fibroblasts. **A** Lung fibroblasts were stimulated for 24 h with either LLC-exo or PBS and inflammatory cytokines in the culture supernatant were detected using mouse cytokine microarrays. **B** CCL1 protein concentrations in LLC-exo stimulated fibroblasts were analyzed by mouse

CCL1 ELISA. **C** *Ccl1* mRNA levels in LLC-exo treated lung fibroblasts were detected by qRT-PCR. **D** CCL1 expression in LLC-exo pre-treated lungs and co-localization with  $\alpha$ -SMA<sup>+</sup> lung fibroblasts were determined by immunofluorescence staining; scale bar, 100  $\mu$ m. Data represent the mean  $\pm$  SD ( $n=5$ ). \*\* $P < 0.01$  (Student's *t*-test)

PMN formation and circulating tumor cell colonization of the lung. For this purpose, mice were injected LLC-exo with/without AZ084 via the tail vein every third day (total of three doses) and scarified on day 9 (Fig. 5A). AZ084 treatment reduced the number of CD4<sup>+</sup>Foxp3<sup>+</sup> Tregs in the lungs of LLC-exo pre-injected mice (Fig. 5B, C). Following combined treatment with LLC-exo and AZ084, we injected LLC cells into mice via the tail vein to explore the engraftment potential of circulating tumor cells in the lung after 21 days (Fig. 5D). Of note, LLC-exo pre-injection remarkably increased the numbers and total area of lung metastatic nodules, while AZ084 treatment inhibited the LLC-exo-induced LLC cell seeding in lung (Fig. 5E, F). Moreover, AZ084 treatment also significantly reduced Treg accumulation in LLC-exo stimulated mouse lungs (Fig. 5G, H). However, there were no significant differences between the control, LLC-exo pre-treatment and combined LLC-exo and

AZ084 groups in terms of the number of B cells, MDSCs and T cells detected in the lungs. These data suggested that CCL1-CCR8 inhibition restrains the formation of the immunologically tolerant PMN and tumor cells metastasis in lung by downregulating Treg differentiation.

### Inhibition of LLC-exo release suppresses PMN formation and LLC metastasis

Having shown that CCR8 blockade reduces Treg differentiation and accumulation in the lung and also hampers colonization of the lungs by circulating LLC cells, we further investigated the effect of blocking exosome secretion from primary tumor cells on circulating tumor cell metastasis to the lung. To accomplish this, we used an established mouse subcutaneous LLC tumor model and the exosome secretion inhibitor GW4869 as shown in Fig. 6A. To avoid the

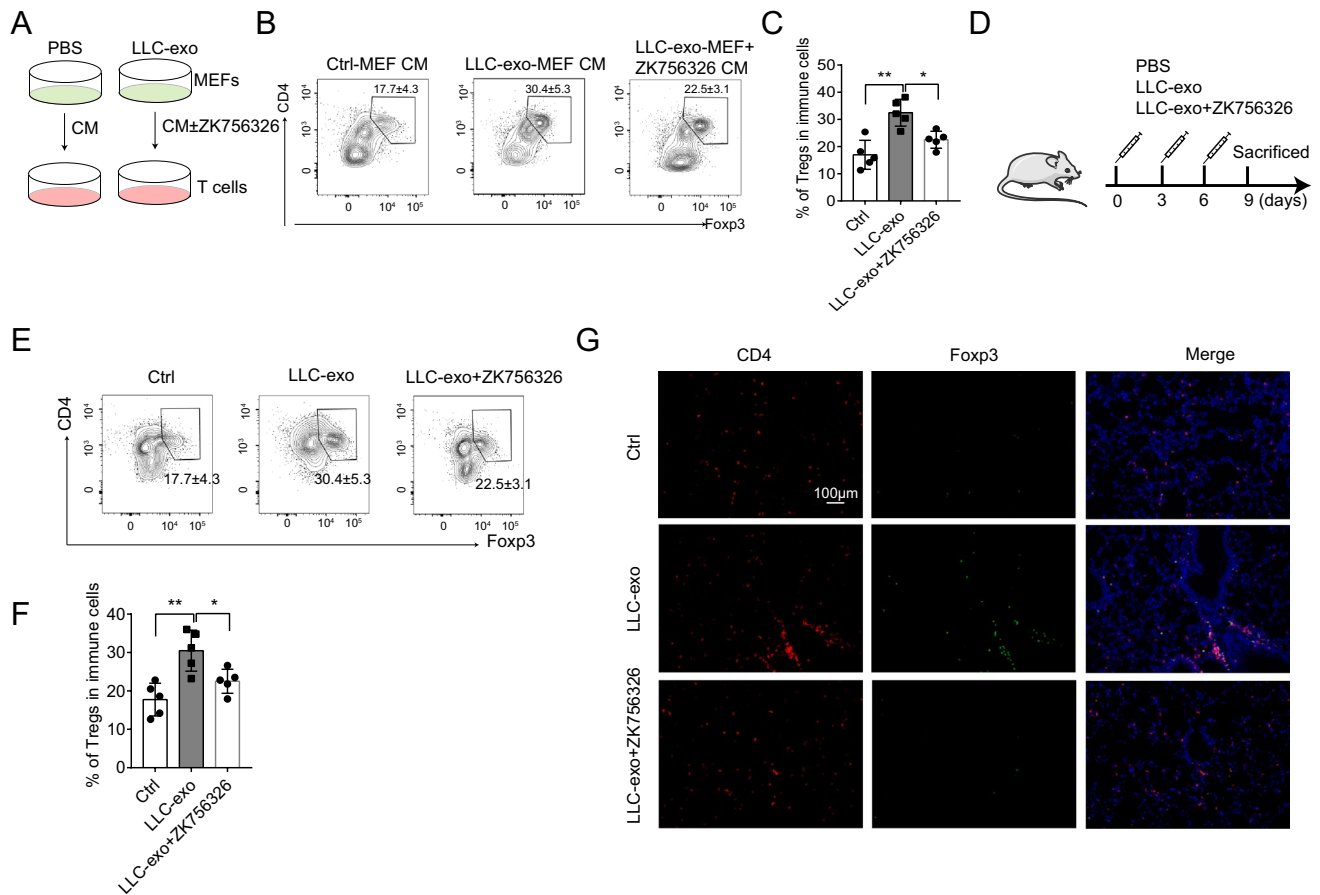


**Fig. 3** LLC-exo induces Treg differentiation via the CCL1-CCR8 axis. **A** MPF were stimulated with either PBS or LLC-exo for 24 h and the culture media were collected (PBS and LLC-exo MPF CM, respectively). Splenic T cells were co-cultured with the LLC-exo MPF CM in the presence and absence of ZK756326 (5  $\mu$ g/ml, daily) for 4 days. **B, C** The number of CD4<sup>+</sup>Foxp3<sup>+</sup> Tregs was analyzed by flow cytometry; data represent the mean  $\pm$  SD ( $n=5$ ). **D** Schematic

diagram of the in vivo LLC-exo MPF CM and ZK756326 treatment experiment. **E, F** The proportion of Tregs in the lungs of mice in each group was determined by flow cytometry; data represent the mean  $\pm$  SD ( $n=5$ ). **G** Immunofluorescence staining of CD4<sup>+</sup>Foxp3<sup>+</sup> Tregs in LLC-exo CM  $\pm$  ZK756326 treated mouse lung: CD4 (red), Foxp3 (green). Nuclei were stained with DAPI. Scale bars, 100  $\mu$ m. \* $P < 0.05$ , \*\* $P < 0.01$  (one-way ANOVA)

interference of continuously secreted exosomes in the late stage of tumor progression, the primary tumor was removed at day 15. Interestingly, there were no significant differences in the volume and growth rate of subcutaneous tumors between the groups treated with GW4869 and AZ084 alone or in combination treatment group and the PBS control group (Fig. 6B, C). However, the number and the area of metastatic nodules generated in the lungs from circulating LLC cells were significantly reduced in both the GW4869 and AZ084 treatment groups. Moreover, the combination of AZ084 and GW4869 further inhibited colonization of the lungs by circulating tumor cells (Fig. 6D–F). Taken together, our findings revealed that primary lung tumor cells contribute to establishment of the PMN to facilitate lung engraftment by circulating tumor cells through transport of exosomes to lung fibroblasts. The mechanism underlying this process involves crosstalk between the lung fibroblasts

and Tregs cells via the CCL1-CCR8 axis, thus creating an immunosuppressive microenvironment that promotes tumor progression.

## Discussion

The function of Tregs in promoting tumor progression has been widely investigated in both animal models and clinical trials [12, 13]. It has been reported that suppressing Treg infiltration or polarization in the TME increases tumor immune responses [26]; however, the accumulation of Tregs in the PMN before tumor cell metastasis has not been systemically explored. In this study, we demonstrated that TDEs play a key role in inducing Treg infiltration into the lung PMN by upregulating fibroblast-derived CCL1 production. Furthermore, inhibiting the release of lung tumor cells



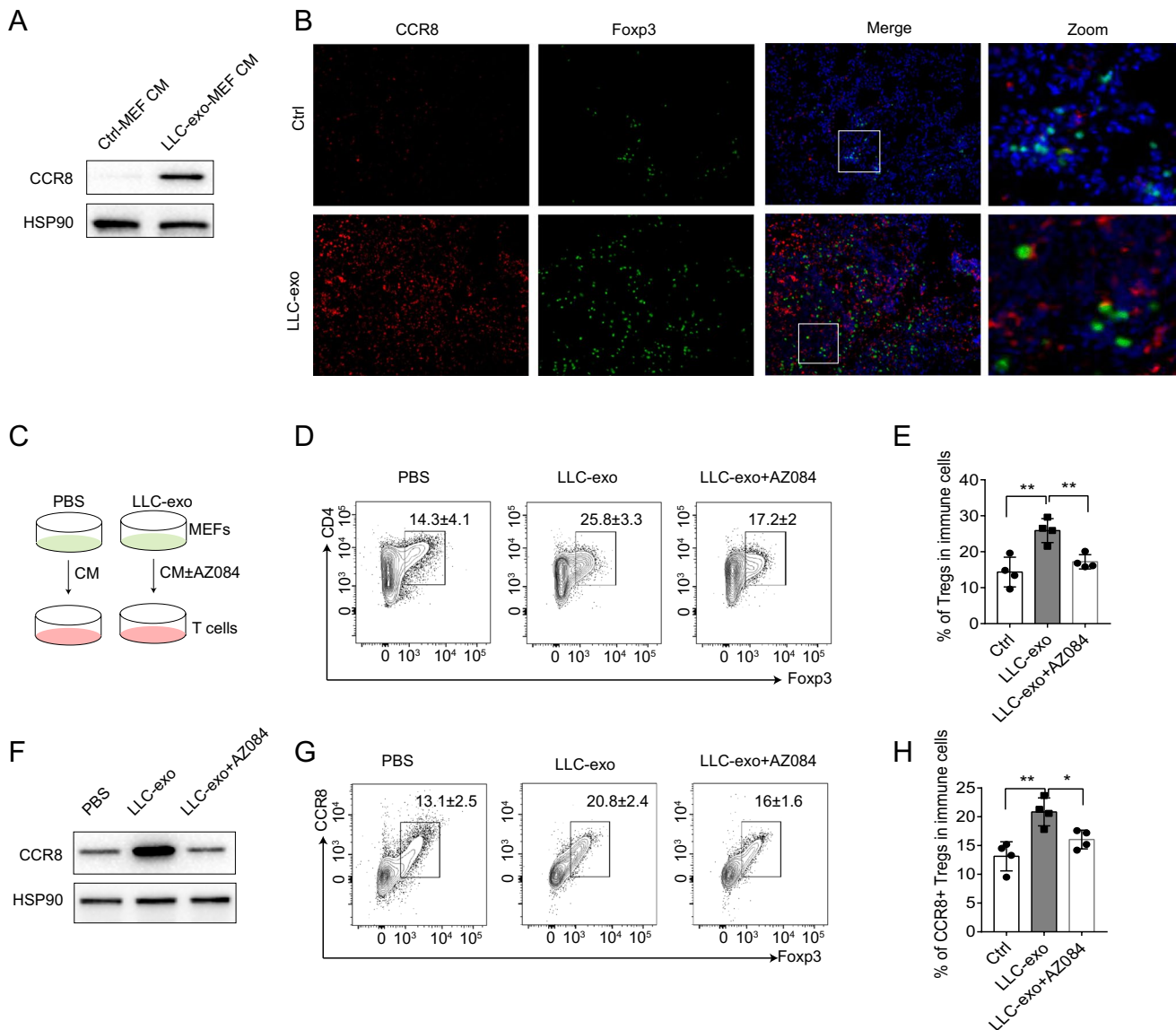


**Fig. 4** CCR8 activation assists Tregs differentiation. **A** Splenic T cells were cultured with LLC-exo stimulated MPF CM for 4 days, and the expression of CCR8 was examined by Western blot analysis; HSP90 was used as a loading control. **B** The co-localization of CCR8 (red) with Foxp3 (green) in the lung of LLC-exo pre-treated mice was determined by immunofluorescence staining. **C–F** Splenic T cells were cultured with LLC-exo MPF CM in the presence and absence

of AZ084 (5 µg/ml, daily) for 4 days. Flow cytometric analysis of CD4<sup>+</sup>Foxp3<sup>+</sup> Treg numbers; data represent the mean ± SD (*n* = 4). **(F)** Western blot analysis of CCR8 expression in splenic T cells treated with LLC-exo MPF CM in the presence and absence of AZ084. **(G–H)** Flow cytometric analysis of CCR8 and Foxp3 co-expression in CD4<sup>+</sup>T cells; data represent the mean ± SD (*n* = 4). \**P* < 0.05, \*\**P* < 0.01 (one-way ANOVA)

exosomes or blocking the CCL1-CCR8 axis suppressed Treg accumulation, and ultimately suppressed circulating tumor cell colonization of the lung.

The anatomical and cellular features of the lung critically underly its ability to receive most circulating tumor cells [27]. The lung is systemically reprogrammed by extrathoracic malignancies including breast and colon cancer, which support the colonization and outgrowth of circulating tumor cells [6]. The immune cells in the lung TME exhibit both pro- and anti-tumoral activities. T lymphocytes, particularly

the CD4<sup>+</sup> and CD8<sup>+</sup> T cells in the TME, exert key effector cytotoxic functions and mediate the tumor killing response. In contrast, MDSCs, which are abundant components of the lung cancer infiltrate, are reported to play an essential role in promoting the PMN formation and tumor metastasis by dampening T cell proliferation, cytokine production, angiogenesis and Treg induction in cancer [28]. However, in our study, we did not observe increased numbers of MDSCs and T cells in the lungs of LLC-exo pre-injected mice. Therefore, we speculate that the MDSCs and T cells in the lungs

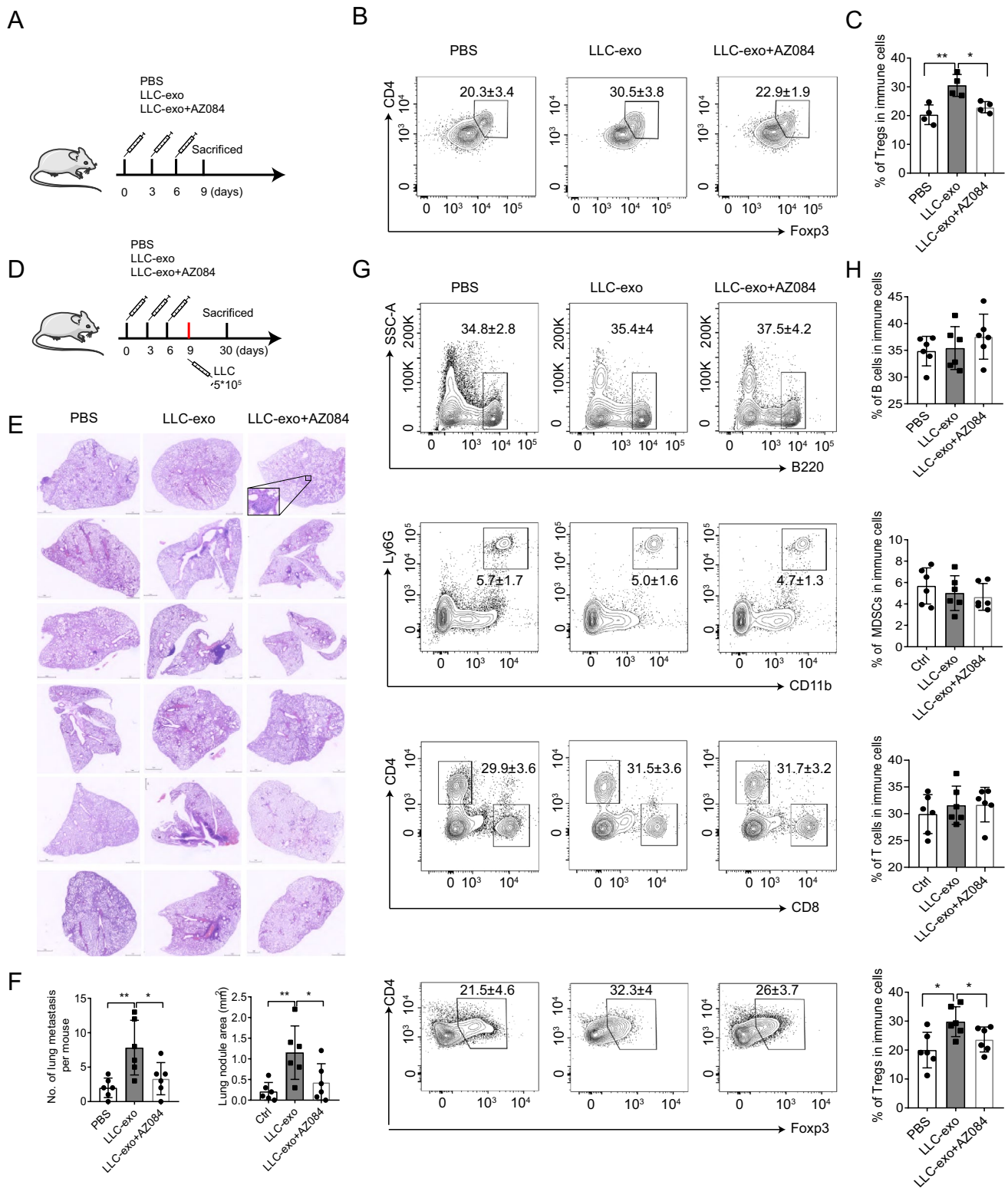


**Fig. 5** AZ084 inhibits Treg differentiation and tumor cell colonization of the lungs. **A** Schematic diagram of the in vivo protocol for treatment of mice with LLC-exo and AZ084. **B, C** Flow cytometric analysis of the number of CD4<sup>+</sup>Foxp3<sup>+</sup> Tregs in lungs; data represent the mean ± SD ( $n=4$ ). **D** Schematic diagram of the in vivo protocol used to evaluate tumor colonization in mice treated with LLC-

exo with/without AZ084. **E, F** HE staining and quantification of the numbers and total area of lung metastatic nodules; data represent the mean ± SD ( $n=4$ ). (**G-H**) Flow cytometric analysis of the immune cells populations (B220<sup>+</sup> B cells, Ly6G<sup>+</sup>CD11b<sup>+</sup>+MDSCs, CD4<sup>+</sup>/CD8<sup>+</sup> T cells and CD4<sup>+</sup>Foxp3<sup>+</sup> Treg); data represent the mean ± SD ( $n=6$ ). \* $P<0.05$ , \*\* $P<0.01$  (one-way ANOVA)

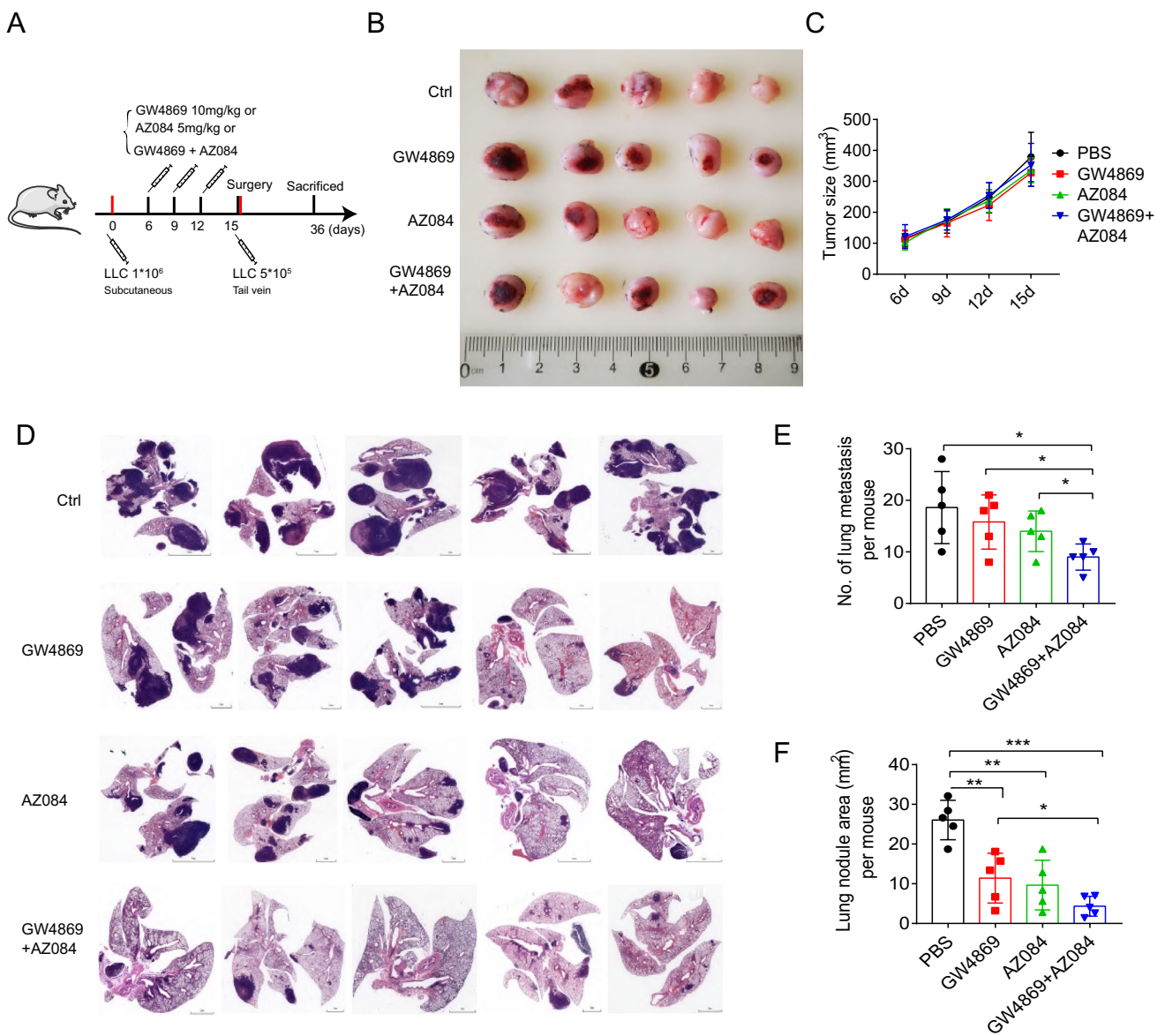


**Fig. 6** Combination of GW4869 and AZ084 significantly reduces tumor cells metastasis in the lungs. **A** Schematic diagram of the protocol for in vivo treatment of mice with GW4869 and ZK756326. LLC cells ( $1 \times 10^6$ ) were subcutaneously injected into mice, and either GW4869 (10 mg/kg) or AZ084 (5 mg/kg) were injected intraperitoneally every 3 days. After surgical removal the LLC tumors at day 15, LLC cells ( $5 \times 10^5$ ) were injected intravenously via the

tail vein. Mice were sacrificed at day 36. **B** The morphology of the tumors at 15 days after treatment. **C** Tumor growth (volume); data represent the mean  $\pm$  SD ( $n=5$ ). **D–F** HE staining and quantification of the numbers and total area of lung metastatic nodules; data represent the mean  $\pm$  SD ( $n=5$ ). \* $P < 0.05$ , \*\* $P < 0.01$ , \*\*\* $P < 0.001$  ( $t$ -test)

of LLC-exo treated mice have limited effects on tumor cell colonization. Moreover, these observations indicate that Treg accumulation in LLC-exo pre-treated mouse lung is not dependent on MDSCs.

Accumulating evidence suggests that Tregs suppress anti-tumor immune responses and influence the efficiency of immunotherapy [13, 29, 30]. In melanoma, gastric cancer and breast cancer, the increased number of Foxp3<sup>+</sup> Tregs in tumor tissue is associated with poor survival and therapeutic

outcome [31, 32]. However, the function of Tregs in lung PMN formation and tumor metastasis remains to be elucidated. We found that the increased number of Tregs in mice pre-treated with LLC-exo was correlated with more metastatic lesions in the lung. Furthermore, inhibition of Treg differentiation reversed circulating tumor cell colonization of the lung. Based on the critical function of Tregs in tumor metastasis, it is noteworthy that removal of Tregs evokes an anti-tumor immune response and improves the outcome of

immunotherapy [12, 13, 33]. Unfortunately, systemic depletion of Tregs will concurrently elicit autoimmune diseases [34]. The current strategy for evoking effective anti-tumor immunity without immune-related adverse events is to specifically target the differentiated functional Tregs, instead of all Foxp3<sup>+</sup> Tregs [13]. CCR4 is predominantly expressed by effector Tregs, but not native Tregs. It has been shown that effector Tregs are effectively depleted by anti-CCR4 antibody treatment without influences on CD4<sup>+</sup>/CD8<sup>+</sup> T cell differentiation [35]. CCR8 is predominantly expressed on Tregs and plays a critical role in Treg-mediated immunosuppression [25]. Treatment with monoclonal anti-CCR8 antibodies has been shown to inhibit tumor growth, enhance anti-tumor immunity and prolong survival in colorectal tumor mouse models [36]. In the current study, we observed that the expression of CCR8 in T cells was upregulated by LLC-exo MPF CM. Moreover, we showed that blockade of the CCL1-CCR8 axis by specific inhibitors (ZK756326 and AZ084, respectively) prevented Treg differentiation both in vitro and in vivo.

Fibroblasts are a predominant component of tumor stroma that have been shown to play an essential role in the processes involved in tumor progression, including invasion and metastasis, although their interactions with other cells, such as immune cells in TME, remain to be defined [37, 38]. It has been reported that Foxp3<sup>+</sup> Treg polarization induced by esophageal cancer-derived cancer-associated fibroblasts (CAFs) is mediated by IL-6. Furthermore, targeting CAFs or IL-6 blockade improved the efficacy of immunotherapy and the pre-existing tumor immunity [39]. However, the role of the interplay between fibroblasts and Tregs in the lung PMN formation is unclear. In this study, we observed that the production of CCL1, but not IL-6 was significantly upregulated in LLC-exo treated lung fibroblasts. CCL1 has been suggested to play a key role in Treg polarization [25]. In addition, as the expression levels of other chemokines, such as CCL2, CCL5, CXCL1 and CXCL12, were not significantly upregulated in LLC-exo treated lung fibroblasts, it can be speculated that the increased number of Tregs was polarized by the local lung environment rather than being recruited from circulating Tregs. We further demonstrated that the fibroblast-derived CCL1 production was remarkably increased by LLC-exo stimulation, which contributed to Treg differentiation in the lung PMN.

A growing body of evidence indicates that TDEs function as communicators and play an essential role in PMN formation, although the underlying mechanism requires further clarification [15, 22]. Liu et al. demonstrated that

tumor exosomal RNAs facilitate the establishment of the lung PMN and primary tumor cell metastasis by activating alveolar epithelial cell TLR3 to induce neutrophil recruitment [40]. In our previous study, we also demonstrated that lung TDE-derived miR-3473b plays a key role in reprogramming lung fibroblasts and promoting pro-inflammatory cytokine production [24]. In the present study, we further confirmed that suppression of TDE production downregulated CCL1 secretion by lung fibroblasts and impeded Treg differentiation, ultimately inhibiting tumor cell lung seeding. Although LLC-exo have propensity to home to the lung, the TDEs from other tumor cells like breast cancer, liver cancer and bladder tumor may also induce the Tregs differentiation and lung PMN formation, which still needs to be further investigated.

In summary, we have demonstrated that the number of Tregs, but not other immune cells such as MDSCs, is remarkably increased in the lungs of LLC-exo pre-treated mice. Our findings indicate that LLC-exo treatment induces a favorable immunosuppressive microenvironment for circulating LLC cell colonization. Mechanistically, we provide evidence that LLC cell-derived TDEs promote CCL1 secretion by lung fibroblasts, which induces Treg differentiation via its receptor, CCR8. Targeting TDE production, as well as blockade of the CCL1-CCR8 axis significantly reduced the number of Tregs in the lung and circulating tumor cell seeding of the lung (Fig. 7). Thus, our study enhances the understanding of the mechanism by which tumor cells regulate lung PMN formation to facilitate tumor cell colonization of the lung, and provides a potential therapeutic target for suppression of lung metastasis from the transitional medicine perspective. The LLC-exo cargo and the potential involvement of other cells in the lung that influence Treg differentiation and PMN formation warrant further investigation. In addition, future studies will clarify the long-term outcomes associated with suppression of lung metastasis by inhibiting TDE secretion or blockade of the CCL-CCR8 axis, either as a monotherapy or in combination.

## Conclusion

In this study, we have illustrated a new molecular mechanism of Treg accumulation in the lung PMN and highlighted a potential therapeutic target for inhibiting cancer cell lung metastasis.



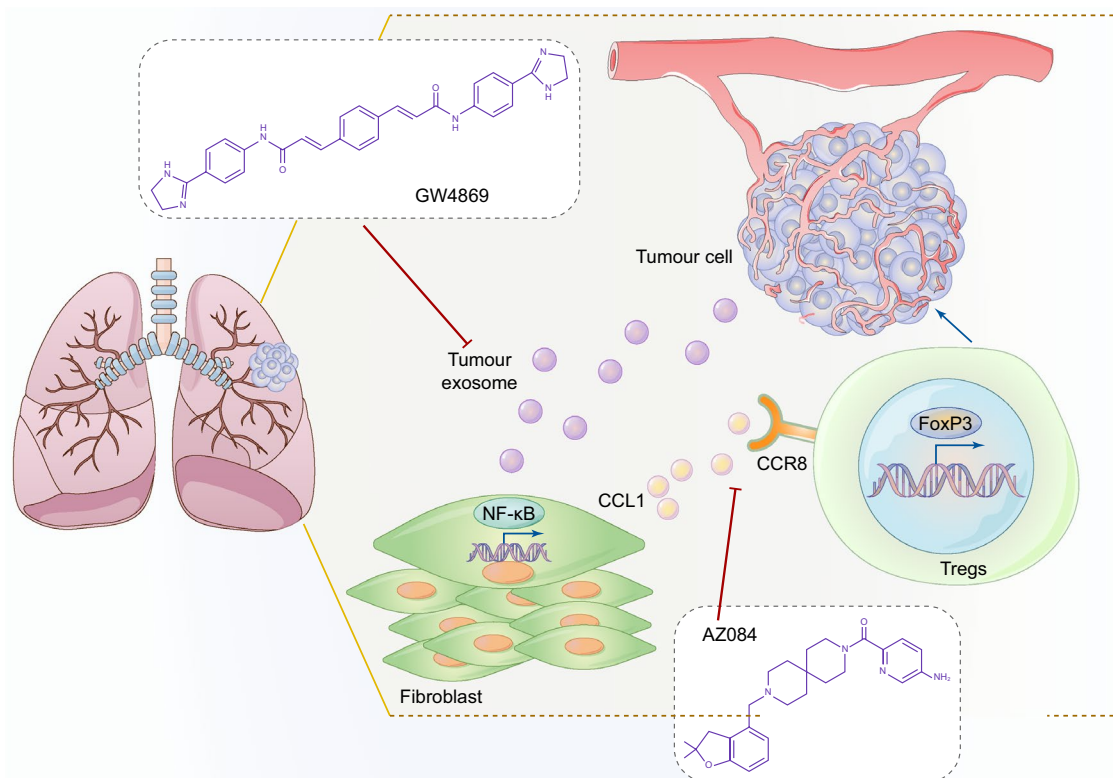


**Fig. 7** Schematic diagram of the proposed mechanism by which TDEs drive tumor cell colonization of the lung via fibroblast CCL1 production and Treg CCR8 activation

**Acknowledgements** We thank Dr. Jessica Tamanini from Insight Editing London for critical reading of the manuscript.

**Author contributions** MW and ZHQ designed the project. MW and ZYQ conducted most of the experiments. YY and XXD performed animal experiments. JJW and XHY responsible for immunofluorescence staining. ZMJ, WQL performed some of the cell culture experiments. MW and ZYQ analyzed the data. MW and ZYQ wrote and edited the manuscript. All authors have read and agreed the contents of the manuscript and consent to its publication.

**Funding** This work was supported by the National Natural Science Foundation of China (Grant Nos. 2021YFA1201102, 82073231) and the Henan Province Scientific and Technological Research (Grant Nos. 222102310728).

**Availability of data and materials** The authors declare that all data and materials are available on request.

## Declarations

**Conflict of interest** The authors declare no competing interests.

**Ethical approval** All animal experiments were approved by the Ethical Review Committee of the First Affiliated Hospital of Zhengzhou University under approval number 2020-KY-154.

**Consent for publication** Not applicable.

## References

- Chaffer CL, Weinberg RA (2011) A perspective on cancer cell metastasis. *Science* 331:1559–1564
- Gupta GP, Massagué J (2006) Cancer metastasis: building a framework. *Cell* 127:679–695
- de Groot AE, Roy S, Brown JS, Pienta KJ, Amend SR (2017) Revisiting seed and soil: examining the primary tumor and cancer cell foraging in metastasis. *Mol Cancer Res* 15:361–370
- Liu Q, Zhang H, Jiang X, Qian C, Liu Z, Luo D (2017) Factors involved in cancer metastasis: a better understanding to “seed and soil” hypothesis. *Mol Cancer* 16:176
- Akhtar M, Haider A, Rashid S, Al-Nabet A (2019) Paget’s, “seed and soil” theory of cancer metastasis: an idea whose time has come. *Adv Anat Pathol* 26:69–74
- Peinado H, Zhang H, Matei IR, Costa-Silva B, Hoshino A, Rodrigues G et al (2017) Pre-metastatic niches: organ-specific homes for metastases. *Nat Rev Cancer* 17:302–317
- Liu Y, Cao X (2016) Characteristics and significance of the pre-metastatic niche. *Cancer Cell* 30:668–681
- Guo Y, Ji X, Liu J, Fan D, Zhou Q, Chen C et al (2019) Effects of exosomes on pre-metastatic niche formation in tumors. *Mol Cancer* 18:39
- Gillot L, Baudin L, Rouaud L, Kridelka F, Noël A (2021) The pre-metastatic niche in lymph nodes: formation and characteristics. *Cell Mol Life Sci* 78:5987–6002
- Dogliani G, Parik S, Fendt SM (2019) Interactions in the (pre) metastatic niche support metastasis formation. *Front Oncol* 9:219



11. Zhuge X, Sun Y, Jiang M, Wang J, Tang F, Xue F et al (2019) Acetate metabolic requirement of avian pathogenic *Escherichia coli* promotes its intracellular proliferation within macrophage. *Vet Res* 50:31
12. Ohue Y, Nishikawa H (2019) Regulatory T (Treg) cells in cancer: Can Treg cells be a new therapeutic target? *Cancer Sci* 110:2080–2089
13. Tanaka A, Sakaguchi S (2017) Regulatory T cells in cancer immunotherapy. *Cell Res* 27:109–118
14. Olkhanud PB, Baatar D, Bodogai M, Hakim F, Gress R, Anderson RL et al (2009) Breast cancer lung metastasis requires expression of chemokine receptor CCR4 and regulatory T cells. *Cancer Res* 69:5996–6004
15. Wortzel I, Dror S, Kenific CM, Lyden D (2019) Exosome-mediated metastasis: communication from a distance. *Dev Cell* 49:347–360
16. Hoshino A, Costa-Silva B, Shen TL, Rodrigues G, Hashimoto A, Tesic Mark M et al (2015) Tumour exosome integrins determine organotropic metastasis. *Nature* 527:329–335
17. Sun W, Ren Y, Lu Z, Zhao X (2020) The potential roles of exosomes in pancreatic cancer initiation and metastasis. *Mol Cancer* 19:135
18. Zhang YF, Zhou YZ, Zhang B, Huang SF, Li PP, He XM et al (2019) Pancreatic cancer-derived exosomes promoted pancreatic stellate cells recruitment by pancreatic cancer. *J Cancer* 10:4397–4407
19. Morrissey SM, Zhang F, Ding C, Montoya-Durango DE, Hu X, Yang C et al (2021) Tumor-derived exosomes drive immunosuppressive macrophages in a pre-metastatic niche through glycolytic dominant metabolic reprogramming. *Cell Metab* 33:2040–58.e10
20. Al-Nedawi K, Meehan B, Kerbel RS, Allison AC, Rak J (2009) Endothelial expression of autocrine VEGF upon the uptake of tumor-derived microvesicles containing oncogenic EGFR. *Proc Natl Acad Sci U S A* 106:3794–3799
21. Fares J, Fares MY, Khachfe HH, Salhab HA, Fares Y (2020) Molecular principles of metastasis: a hallmark of cancer revisited. *Signal Transduct Target Ther* 5:28
22. Zhang L, Yu D (2019) Exosomes in cancer development, metastasis, and immunity. *Biochim Biophys Acta Rev Cancer* 1871:455–468
23. Olejarz W, Dominiak A, Żohnierzak A, Kubiak-Tomaszewska G, Lorenc T (2020) Tumor-derived exosomes in immunosuppression and immunotherapy. *J Immunol Res* 2020:6272498
24. Du C, Duan X, Yao X, Wan J, Cheng Y, Wang Y et al (2020) Tumour-derived exosomal miR-3473b promotes lung tumour cell intrapulmonary colonization by activating the nuclear factor- $\kappa$ B of local fibroblasts. *J Cell Mol Med* 24:7802–7813
25. Barshesht Y, Wildbaum G, Levy E, Vitsenshtein A, Akinseye C, Griggs J et al (2017) CCR8(+)FOXP3(+) T(reg) cells as master drivers of immune regulation. *Proc Natl Acad Sci U S A* 114:6086–6091
26. Nishikawa H, Koyama S (2021) Mechanisms of regulatory T cell infiltration in tumors: implications for innovative immune precision therapies. *J Immunother Cancer*. <https://doi.org/10.1136/jitc-2021-002591>
27. Altorki NK, Markowitz GJ, Gao D, Port JL, Saxena A, Stiles B et al (2019) The lung microenvironment: an important regulator of tumour growth and metastasis. *Nat Rev Cancer* 19:9–31
28. Wang Y, Ding Y, Guo N, Wang S (2019) MDSCs: key criminals of tumor pre-metastatic niche formation. *Front Immunol* 10:172
29. Li C, Jiang P, Wei S, Xu X, Wang J (2020) Regulatory T cells in tumor microenvironment: new mechanisms, potential therapeutic strategies and future prospects. *Mol Cancer* 19:116
30. Yano H, Andrews LP, Workman CJ, Vignali DAA (2019) Intratumoral regulatory T cells: markers, subsets and their impact on anti-tumor immunity. *Immunology* 157:232–247
31. Kim JH, Kim BS, Lee SK (2020) Regulatory T Cells in tumor microenvironment and approach for anticancer immunotherapy. *Immune Netw*. <https://doi.org/10.4110/in.2020.20.e4>
32. deLeeuw RJ, Kost SE, Kakal JA, Nelson BH (2012) The prognostic value of FoxP3+ tumor-infiltrating lymphocytes in cancer: a critical review of the literature. *Clin Cancer Res* 18:3022–3029
33. Paluskiewicz CM, Cao X, Abdi R, Zheng P, Liu Y, Bromberg JS (2019) T regulatory cells and priming the suppressive tumor microenvironment. *Front Immunol* 10:2453
34. Sakaguchi S (2004) Naturally arising CD4+ regulatory t cells for immunologic self-tolerance and negative control of immune responses. *Annu Rev Immunol* 22:531–562
35. Sugiyama D, Nishikawa H, Maeda Y, Nishioka M, Tanemura A, Katayama I et al (2013) Anti-CCR4 mAb selectively depletes effector-type FoxP3+CD4+ regulatory T cells, evoking anti-tumor immune responses in humans. *Proc Natl Acad Sci USA* 110:17945–17950
36. Villarreal DO, L'Huillier A, Armington S, Mottershead C, Filipova EV, Coder BD et al (2018) Targeting CCR8 induces protective antitumor immunity and enhances vaccine-induced responses in colon cancer. *Cancer Res* 78:5340–5348
37. Kalluri R (2016) The biology and function of fibroblasts in cancer. *Nat Rev Cancer* 16:582–598
38. Sahai E, Astsaturov I, Cukierman E, DeNardo DG, Egeblad M, Evans RM et al (2020) A framework for advancing our understanding of cancer-associated fibroblasts. *Nat Rev Cancer* 20:174–186
39. Kato T, Noma K, Ohara T, Kashima H, Katsura Y, Sato H et al (2018) Cancer-associated fibroblasts affect intratumoral CD8(+) and FoxP3(+) T cells Via IL6 in the tumor microenvironment. *Clin Cancer Res* 24:4820–4833
40. Liu Y, Gu Y, Han Y, Zhang Q, Jiang Z, Zhang X et al (2016) Tumor exosomal RNAs promote lung pre-metastatic niche formation by activating alveolar epithelial TLR3 to recruit neutrophils. *Cancer Cell* 30:243–256

**Publisher's Note** Springer Nature remains neutral with regard to jurisdictional claims in published maps and institutional affiliations.